

Anomalous Surface Phonon Dispersion Relations for Ag(111) Measured by Inelastic Scattering of He Atoms

R. B. Doak

Bell Telephone Laboratories, Murray Hill, New Jersey 07974

and

U. Harten and J. Peter Toennies

Max-Planck-Institut für Strömungsforschung, D-3400 Göttingen, Federal Republic of Germany

(Received 6 April 1983)

High-resolution time-of-flight measurements of 17-meV He atoms scattered from an Ag(111) surface along the $\langle 11\bar{2} \rangle$ and $\langle 110 \rangle$ azimuths are reported. Most of the spectra reveal two sharp peaks and from their locations dispersion curves have been determined out to the zone boundary. The agreement of the lower-frequency mode with the theoretical Rayleigh dispersion curve is excellent. The other mode is significantly lower (35%) than the calculated longitudinally polarized surface mode.

PACS numbers: 68.25.+j, 63.20.Dj, 79.20.Rf

In 1981 we reported high-resolution inelastic time-of-flight (TOF) scattering experiments of 20-meV He atoms from LiF crystals along the $\langle 100 \rangle$ azimuth.^{1,2} The results provided the first accurate measurement of the surface phonon Rayleigh-mode dispersion curve $\omega(Q)$ out to the zone boundary. The agreement with the well-developed theory for ionic crystals was good except at the zone boundary where the measured frequency was about 10% lower than predicted. Since then dispersion curves have been reported for (001) surfaces of LiF $\langle 110 \rangle$,² NaF $\langle 100 \rangle$,² KCl $\langle 100 \rangle$,² and MgO $\langle 100 \rangle$.³ Only in the case of MgO was there a substantial coupling to the bulk modes relative to the Rayleigh mode.

Previous inelastic He-atom scattering experiments on metals were reported by Yerkes and Miller⁴ from Ag(111) and by Mason and Williams⁵ from Cu(100) at 16 K. The latter authors observed phonon interactions out to over halfway to the zone boundary. One set of points was attributed to a linear Rayleigh dispersion, while the other points were on or above the transverse bulk dispersion curve. Recently Cates and Miller⁶ reported time-of-flight spectra for epitaxial Au(111) out to the zone boundary ($\langle 11\bar{2} \rangle$), but could only resolve what appeared to be the Rayleigh mode. Feuerbacher and Willis⁷ have studied the inelastic scattering of He and Ne atoms from Ni(111). They attributed the inability to see single-phonon interactions beyond $Q/Q_m \approx 0.6$ with Ne to a "cutoff" resulting from the large interaction radius of Ne atoms. Simultaneously with the present experiments, Lehwald *et al.*⁸ have used inelastic electron scattering with a resolution of 7 meV to measure surface phonon dispersion re-

lations for Ni(100) out to the zone boundary. The resolution in the present experiments is better than in previous work on metal surfaces.

The new apparatus⁹ is similar to that used earlier.² The angle between incident and outgoing beams was also fixed at 90° ($= \theta_i + \theta_f$) and the incident angle θ_i (with respect to the surface normal) was changed by rotating the crystal. The He beam had an energy of 17.5 meV ($k_i = 5.76 \text{ \AA}^{-1}$) and a velocity resolution of $\Delta v/v = 1.2\%$. The overall apparatus resolution is ΔE (full width at half maximum) = 0.4 meV. The distance from chopper to target was 0.390 m and from target to detector, 1.230 m. The crystal was mounted in a compact UHV target chamber with a base pressure of 10^{-11} Torr. Two Ag(111) crystals were used. The first was a solid single crystal prepared by mechanical polishing, chemical etching, and finally sputtering and annealing in vacuum until a satisfactory Auger spectrum and low-energy electron-diffraction picture were obtained. The observation of small (10^{-4} of specular intensity) first-order diffraction peaks as reported previously^{10,11} provided further evidence for a smooth single-crystal surface. Additional unidentified peaks were sometimes observed which depended on crystal pretreatment and had no effect on the TOF spectrum. The second crystal, a 1000-Å-thick epitaxially grown layer on mica,¹² did not show these unidentified peaks. In most experiments the crystals were cooled to 140 K.

Figures 1 and 2 show a series of TOF spectra taken on both sides of the specular peak at $\theta_i = 45^\circ$ along the $\langle 11\bar{2} \rangle$ and $\langle 110 \rangle$ azimuths. Arrows above the spectra indicate the significant inelastic structures, and those at the bottom, the inco-

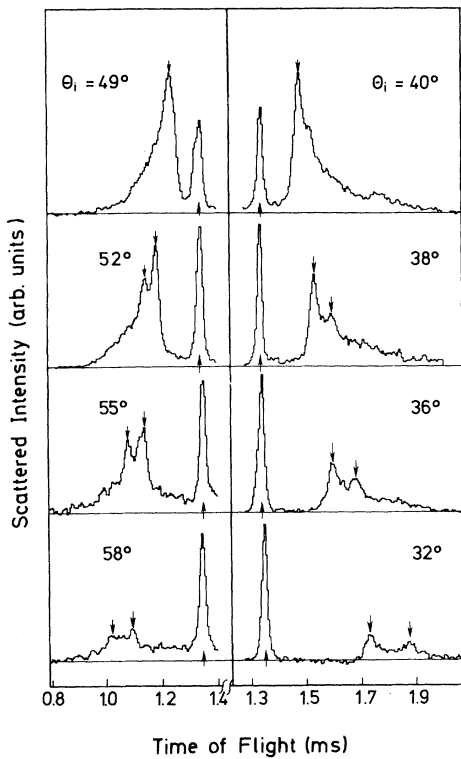


FIG. 1. Several TOF spectra for the $\langle 11\bar{2} \rangle$ azimuth with target at 140 K. The actual signal in counts per channel is plotted vs the measured time of flight. The total measuring time for one spectrum was between $\frac{1}{4}$ and 7 h. The significant inelastic structures and the incoherent elastic peak are indicated on each TOF spectrum by an arrow above and below, respectively. Note that as the angle moves away from the specular ($\theta_i = 45^\circ$), regions of the phonon spectrum with greater $|\vec{Q}_\perp|$ and $|\hbar\omega|$ are probed.

herent elastic peak attributed to crystal imperfections. The first sharp inelastic peak, or, in some cases, plateau edge, was attributed to the surface Rayleigh mode; the other maxima lie in the bulk region. Identical results were obtained with the epitaxially grown crystal.

By assuming the sharp structures to be due to an interaction with single phonons, their energy was determined from the observed TOF differences and the corresponding parallel surface momenta were determined from the incident and final angles via conservation of energy and momentum.² Note that the spectra are simpler than previously observed for LiF since "umklapp" phonons associated with the diffraction peaks are too weak to be seen. Moreover the conditions are such that essentially only phonons with $\omega > 0$, $Q < 0$ and $\omega < 0$, $Q > 0$ (for sign conventions see Refs. 1 and 2) are observed for $\theta_i > 45^\circ$ and $< 45^\circ$, re-

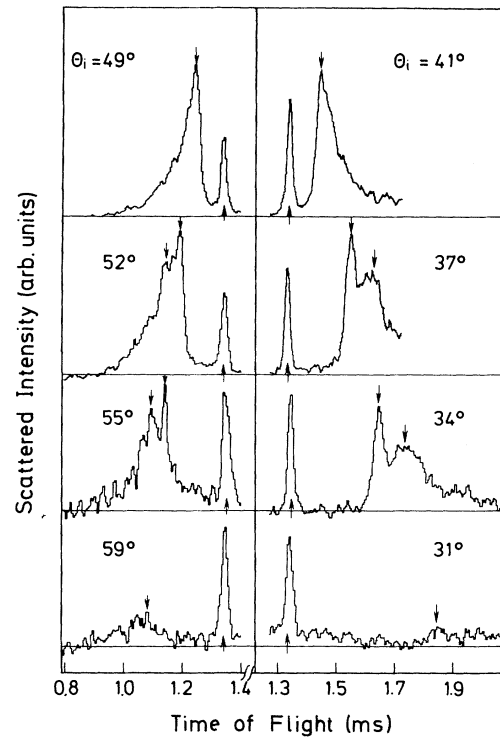


FIG. 2. Same as Fig. 1 but for the $\langle 110 \rangle$ azimuth.

spectively. Figure 3 shows a reduced-zone plot of all the phonon energies and surface momenta determined from a total of 63 measurements for both crystals.

For comparison the calculated surface phonon dispersion relations of Armand¹² are shown, using a maximum frequency of 4.71×10^{12} Hz. The symbols X, Y, Z refer to the surface-mode polar-

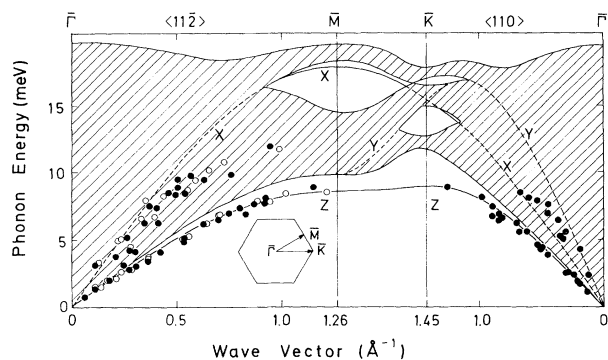


FIG. 3. Reduced-zone plot of the data points (filled circles, solid crystal; open circles, epitaxial crystal). The surface dispersion curves are those calculated by Armand (Ref. 12); those of Bortolani *et al.* (Ref. 13) are similar. The dashed curves are resonances involving surface and bulk modes (1 meV = 0.2418×10^{12} Hz).

ization (OZ normal to the surface, OX and OY parallel to the $\langle 11\bar{2} \rangle$ and $\langle 110 \rangle$ azimuths). Similar calculations for $\langle 11\bar{2} \rangle$ have been made by Bortolani, Nizzoli, Santoro, and Franchini¹³ (BNSF) and by Black, Shanes, and Wallis¹⁴ (BSW). The difference in these calculations can be characterized by the \bar{M} -point Rayleigh and lowest surface-projected bulk mode frequencies (in 10^{12} Hz): Armand, 2.08 and 2.39; BNSF, 2.01 and 2.24; BSW, 2.09–2.42 and 2.32–2.82, respectively. These calculations agree with the measured lower-frequency dispersion curves to within experimental error. The good agreement of Armand's calculation with experiment is surprising since he includes only central forces between nearest neighbors, whereas in the 69-layer-slab BNSF calculation both central and angular forces to second-nearest neighbors are included.

The higher-frequency dispersion curves lie significantly below the longitudinally polarized acoustic mixed mode (LA) denoted by X along the $\langle 11\bar{2} \rangle$ azimuth and by Y along the $\langle 110 \rangle$ azimuth.¹⁵ One possible explanation of this second mode is that it is due to multiphonon events. We rule this out for two reasons: (1) Multiphonon processes will be more probable for the lower-frequency Rayleigh mode and if present would shift this towards smaller Q ,¹⁶ which is not observed. (2) In analogous experiments on Cu(100) with lower resolution, Mason and Williams⁵ appear to have seen a similar process at 16 K where multiphonon processes are much less likely. Thus we associate these higher-frequency modes with the LA mixed mode and seek a reason for the drastic lowering compared to theory.

First we note that in analogous He-atom experiments the LA mixed surface mode has recently been seen in NaF, where its dispersion curve is in reasonable agreement with theory.¹⁷ Moreover, according to LEED experiments Ag(111) shows no structural relaxation.¹⁸ This suggests that the lowering is a dynamic feature of the Ag(111) surface. Since surface electronic states exist only near the $\bar{\Gamma}$ point,¹⁹ nonadiabatic effects such as the Kohn anomaly probably are not a significant factor at large Q values. Bilz²⁰ has suggested that the lowering may be due to the strong quadrupole deformability of Ag ions,²¹ which is related to the low value of the C_{44} force constant in bulk silver. Since at the surface the electronic charge can distort into the vacuum and is not constrained by neighbors on all sides as in the bulk, this effect could be greatly enhanced at the surface. It has not been included in the theo-

retical calculations. A similar effect of ionic deformability has been found in high-temperature superconductors YS, NbN, and $\text{Sm}_{0.75}\text{Y}_{0.25}\text{S}$ where the breathing deformability of the S ion leads to a lowering of the LA bulk mode without effecting the TA mode.²² To check this hypothesis we plan to carry out analogous experiments on Cu(111) and Au(111). Recent experiments in Ni(100),²³ for which the ion deformability is normal, do not show this effect, in agreement with the model of Bilz.

Finally we note that the intensity of the inelastic Rayleigh peak in the TOF spectra decreases rapidly with increasing parallel momentum (and thus energy) exchange. The observed decrease is roughly exponential for the Rayleigh maxima, dropping from $I/I_0 \approx 2 \times 10^{-3}$ at $Q = 0$ to $\approx 1 \times 10^{-5}$ at $|Q| = 1 \text{ \AA}^{-1}$, I_0 being the specular beam intensity. This behavior has been recently explained as due to deformation of the potential by phonon-induced displacements of the surface atoms^{24,25} and provides information on the range of the coupling potential.

We thank A. Gitter for preparing the crystal, C. Wöll for help with the measurements and data evaluation, and G. Armand, R. F. Wallis, and V. Bortolani for communicating their results prior to publication. We are grateful to G. Benedek, H. Bilz, and H. Neddermeyer for several enlightening discussions.

¹G. Brusdeylins, R. B. Doak, and J. P. Toennies, *Phys. Rev. Lett.* **46**, 437 (1981).

²G. Brusdeylins, R. B. Doak, and J. P. Toennies, *Phys. Rev. B* **27**, 3662 (1983).

³G. Brusdeylins, R. B. Doak, J. G. Sokronick, and J. P. Toennies, *Surf. Sci.* **128**, 191 (1983).

⁴S. C. Yerkes and D. R. Miller, *J. Vac. Sci. Technol.* **17**, 126 (1980).

⁵B. F. Mason and B. R. Williams, *Phys. Rev. Lett.* **46**, 1138 (1981), and *J. Chem. Phys.* **75**, 2199 (1981).

⁶M. Cates and D. R. Miller, in *Proceedings of the Third International Conference on Vibrations at Surfaces*, Asilomar, California, August 1982 [*J. Electron Spectrosc. Relat. Phenom.* (to be published)].

⁷B. Feuerbacher and R. F. Willis, *Phys. Rev. Lett.* **47**, 526 (1981).

⁸S. Lehwald, J. M. Szeftel, H. Ibach, T. S. Rahman, and D. L. Mills, *Phys. Rev. Lett.* **50**, 518 (1983).

⁹G. Lilienkamp and J. P. Toennies, *J. Chem. Phys.* **78**, 5210 (1983).

¹⁰G. Boato, P. Cantini, and R. Tatarek, *J. Phys. F* **6**, L237 (1976).

¹¹J. M. Horne and D. R. Miller, *Surf. Sci.* **66**, 365

(1977).

¹²G. Armand, to be published.

¹³V. Bortolani, A. Franchini, F. Nizzoli, and G. Santoro, to be published.

¹⁴J. E. Black, F. C. Shanes, and R. F. Wallis, to be published.

¹⁵R. E. Allen, G. P. Alldredge, and F. W. de Wette, Phys. Rev. B 4, 1661 (1971).

¹⁶H. D. Meyer, R. Rechsteiner, and J. P. Toennies, to be published.

¹⁷G. Benedek, G. Brusdeylins, R. Rechsteiner, J. Skofronick, and J. P. Toennies, to be published.

¹⁸F. Forstmann, Jpn. J. Appl. Phys. Suppl. 2, Pt. 2, 657 (1974); F. Sorio, J. L. Sacedon, P. M. Echenique, and D. Titterington, Surf. Sci. 68, 448 (1977); T. C. Ngoc, M. G. Lagally, and M. B. Webb, Surf. Sci. 35,

117 (1973).

¹⁹P. Heimann, H. Neddermeyer, and H. F. Roloff, J. Phys. C 10, L17 (1977).

²⁰H. Bilz, private communication.

²¹K. Fisher, H. Bilz, R. Haberkorn, and W. Weber, Phys. Status Solidi (b) 54, 285 (1972); W. G. Kleppmann and W. Weber, Phys. Rev. B 20, 1669 (1979).

²²H. Bilz, G. Güntherodt, W. Kleppmann, and W. Kress, Phys. Rev. Lett. 43, 1998 (1979); W. Kress, H. Bilz, G. Güntherodt, and A. Jayaramann, J. Phys. (Paris), Colloq. 42, C6-3 (1981).

²³R. B. Doak, U. Harten, J. P. Toennies, and Ch. Wöll, to be published.

²⁴N. Garcia and J. M. Soler, Surf. Sci. 126, 689 (1983).

²⁵G. Benedek, V. Celli, R. B. Doak, U. Harten, and J. P. Toennies, to be published.